

## Water vapor solubility of poly(lactic acid) films modified the surface by vacuum ultraviolet irradiation

Takuya Saiga, Shuichi Sato, Kazukiyo Nagai

Department of Applied Chemistry, Meiji University, 1-1-1 Higashi-mita, Tama-ku, Kawasaki 214-8571, Japan

Correspondence to: K. Nagai (E-mail: nagai@meiji.ac.jp)

**ABSTRACT:** Surface modification of poly(lactic acid) (PLA) film is performed via 172 nm excimer lamp irradiation. Effects on water vapor solubility and physical properties via vacuum ultraviolet (VUV) irradiation are studied systematically. After VUV irradiation, water vapor solubility increases approximately 11–43% in the low-pressure region and approximately 20–38% in the high-pressure region as surface hydrophilicity increased. The increase is attributed to hydrogen bonding with the carboxyl groups because of VUV radiation. The modified layer is significantly swelling after water vapor sorption. The hydrophilic layer forms a thickness of 2–3  $\mu\text{m}$  from the irradiated surface via VUV radiation, but no changes are observed inside the irradiated film. Therefore, PLA film solubility after irradiation is enhanced by hydrophilicity and the swelling effect of the surface. © 2015 Wiley Periodicals, Inc. *J. Appl. Polym. Sci.* **2015**, *132*, 42200.

**KEYWORDS:** biodegradable; films; photochemistry; polyesters; surfaces and interfaces

Received 11 December 2014; accepted 12 March 2015

DOI: 10.1002/app.42200

### INTRODUCTION

Poly(lactic acid) (PLA) is an environment-friendly biodegradable polymer substance with a low melting point, high moldability, and high transparency. PLA is used in food packaging, electronics, and automobile applications. The water vapor transport property is essential to protecting the contents from water vapor and preventing material degradation (e.g., oxidation and hydrolysis) upon exposure to air. The transport properties of PLA films have been reported in our previous study.<sup>1</sup> Surface modification technologies have been extensively used in material industrial fields and have key functions in improving a wide range of materials.<sup>2</sup> Surface modification via ultraviolet irradiation has been applied to polymers, glasses, ceramics, and metals.<sup>3</sup> This method can be modified using a vacuum ultraviolet (VUV) light emitted from excimer lamps; selective surface oxidation is possible because the wavelength light of 172 nm is completely absorbed in the polymer material. Therefore, VUV irradiation is a possible modification method for hydrophilicity only the polymer surface.<sup>4,5</sup> Unlike plasma irradiation, VUV irradiation via excimer lamps is performed at atmospheric pressures and low temperatures. Surface modification technology is generally used to develop methods for material adhesion and surface cleaning.<sup>6–8</sup> Figure 1 shows that PLA film adhesion to plastic film can be increased through an adhesiveless process occurring under atmospheric pressure. Adhesive use in organic solvents causes problems in the touch panels of liquid crystal

displays and solar battery panels because water and organic solvents degrade the performances of these devices. Therefore, adhesiveless processes are necessary for next-generation electronic devices.

The effects of VUV irradiation on bulk, surface, and water vapor permeation properties of PLA films and on their structures have been evaluated in our previous study.<sup>4</sup> Figure 2 presents the schematics of Norrish type II reaction via VUV irradiation.<sup>9,10</sup> Hydrophilicity was increased by the photodegradation reaction through the Norrish mechanism, which generated OH groups on the PLA surface. Simultaneously, we employed water contact angle and observed that VUV irradiation increased hydrophilicity. Water vapor permeability of the PLA film after irradiation was the same before irradiation. However, mechanisms based on the true value of water vapor solubility of VUV-irradiated PLA for improving adhesion have not been reported. Unlike gas molecules (e.g., nitrogen and oxygen), interactions between water and polymer and between water molecules significantly affect water vapor permeability. Water vapor solubility to PLA is determined by measuring the sorption properties. These PLA interactions would be stronger through hydrophilic treatment. Therefore, a systematic study of water vapor sorption properties is important to discussing the water vapor permeation mechanism of PLA films. Consequently, we systematically investigate the VUV irradiation effects on solubility and surface structure of PLA films.

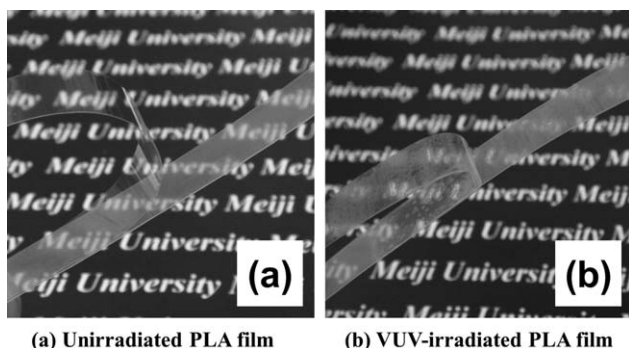


**Figure 1.** Adhesion of the plastic film to (a) unirradiated and (b) VUV-irradiated PLA films.

## EXPERIMENTAL

### Film Preparation

We used the same PLA films from our previous study.<sup>1</sup> The PLA polymer had a 4032D product (NatureWorks LLC, Minnetonka). The isomer ratio ranged from  $L:D = 96.0 : 4.0$ – $96.8 : 3.2$ . PLA films were prepared by casting 2 wt % dichloromethane solution of each solvent on to a flat-bottomed petri dish in a glass bell-type vessel, which were then dried under atmospheric pressure at room temperature. Each solvent was allowed to evaporate for 48 h. The dried PLA films were then thermally treated under vacuum for 48 h at  $70^{\circ}\text{C}$  to completely eliminate the residual solvent and obtain amorphous PLA films. The thermally treated PLA films were then cooled at room temperature under atmospheric pressure. Proton nuclear magnetic resonance ( $^1\text{H-NMR}$ ) (JNM-ECA500, JEOL) analysis was used to confirm the removal of the residual solvent. Film thickness varied from  $35\ \mu\text{m}$  to  $45\ \mu\text{m}$ , and the uncertainty of each film thickness was  $\pm 1\ \mu\text{m}$ .

### VUV Irradiation

VUV irradiation via excimer light was conducted in the same manner as the method in our previous study.<sup>4</sup> VUV excimer lamp irradiation was performed with an excimer VUV light emission unit (UER20H-172 V, Ushio). The radiation wavelength was 172 nm, and irradiance was from 2 to  $3\ \text{mW}/\text{cm}^2$ . The distance between the excimer lamp and PLA film was approximately 20 mm. The contact angle contributed to water vapor solubility. VUV irradiation was performed on only one side of each PLA film for 60 min at  $23 \pm 1^{\circ}\text{C}$ ; the water contact angle reached a steady state at this irradiation time in our previous study. The VUV-irradiated PLA films were then kept in a vacuum, and their sorption properties were measured within 48 h.

### Measurement of Water Vapor Sorption

Sorption data were determined in the film state for at least three samples to confirm the reproducibility of the experimental results. Water vapor sorption in PLA films were gravimetrically determined as a function of pressure at  $25 \pm 1$ ,  $35 \pm 1$ , and  $45 \pm 1^{\circ}\text{C}$  using a calibrated helical quartz spring sorption system.<sup>11,12</sup> The sorption system was removed after 12 h at the same measurement temperature when the sample was introduced to degas the PLA film. Ultrapure water is utilized as water vapor to remove the dissolved gases by freeze drying.

Water vapor was introduced at a fixed pressure. The resulting change in spring extension was monitored with differential transformer transducers and recorded for up to 3.8 cm Hg as a function of time. The saturated vapor pressure ( $p_{\text{sat}}$ ) values were 2.38 cmHg at  $25^{\circ}\text{C}$ , 4.23 cmHg at  $35^{\circ}\text{C}$ , and 7.21 cmHg at  $45^{\circ}\text{C}$ .<sup>13</sup> The experiments were performed according to increasing relative pressure ( $p/p_{\text{sat}}$ ) with specific intervals.  $p/p_{\text{sat}}$  was provided stepwise from 0 to 0.9. The equilibrium concentration of water vapor sorption was calculated as follows:<sup>14</sup>

$$C = 22414 \times \frac{m_s \rho_p}{m_p MW_s} \quad (1)$$

where  $C$  is concentration of water vapor sorption [ $\text{cm}^3(\text{STP})/\text{cm}^3$  (polymer)],  $m_p$  is the polymer mass (g),  $m_s$  is the penetrant mass in the polymer (g),  $\rho_p$  is the polymer density ( $\text{g}/\text{cm}^3$ ),  $MW_s$  is the penetrant molecular weight (g/mol), and 22,414 is a conversion factor [ $\text{cm}^3(\text{STP})/\text{mol}$ ].

### Characterization Analysis

All characterization data were determined in at least three film samples to confirm the reproducibility of the experimental results.

Wide-angle X-ray diffraction (WAXD) measurement was performed using a Rint 1200 X-ray diffractometer (Rigaku, Corp.) with a Cu-K $\alpha$  radiation source at 40 kV and 20 mA in a dispersion angle of  $3.00^{\circ}$  to  $30.00^{\circ}$  and a scanning speed of  $2^{\circ}/\text{min}$  at  $23 \pm 1^{\circ}\text{C}$ . The  $d$ -spacing was calculated according to Bragg's conditions (2), which presented the mean distance between polymer chains:

$$\lambda = 2d \sin \theta \quad (2)$$

where  $\lambda$  is the X-ray wavelength (1.54 Å) and  $d$  is distance of lattice spacing (Å). Moreover, the value of  $\theta$  was the diffraction angle at peak maximum intensity determined from the Gauss function.

Scanning electron microscopy (SEM) was performed with a high-resolution field emission SEM (FE-SEM) (S5200, Hitachi High-Technologies Corporation, Tokyo, Japan). The SEM sample was prepared by surface coating with a magnetron-type ion-sputtering instrument (JCS-1600, JEOL, Ltd., Tokyo, Japan). The sample was coated with platinum at 70 s and 30 mA. The acceleration voltage of the SEM was 5 kV.

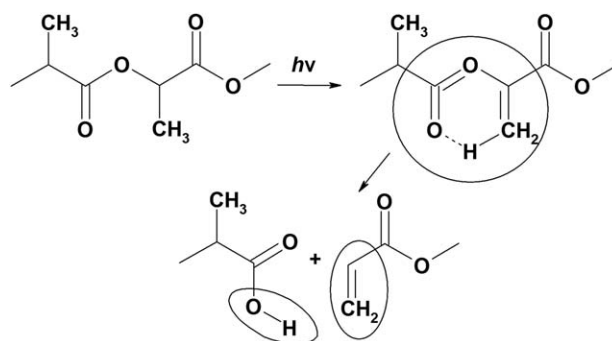


**Figure 2.** Norrish type II mechanism for PLA photodecomposition: chain of PLA under VUV irradiation, photophysical excitation, and scission reactions in PLA chains.

Orthoscope observation was performed using an Olympus BX-51 polarization microscope (POM) (Olympus Inc., Tokyo, Japan) at cross Nicol condition. Polarization images were observed under an additive color with a sensitive color plate at 530 nm.

Attenuated total reflectance (ATR) Fourier transform infrared (FTIR) spectra were obtained with FT/IR-4100 and ATR-PRO450-S (JASCO Co., Tokyo, Japan) using the HATR ZnSe 45° flat plate (PIKE Technologies, Watertown). The incidence angle was set at 45°, resolution was 2 cm<sup>-1</sup>, cumulated number was 32 times, measuring temperature was 23 ± 1°C, and relative humidity was 50 ± 5%RH.

## RESULTS AND DISCUSSION

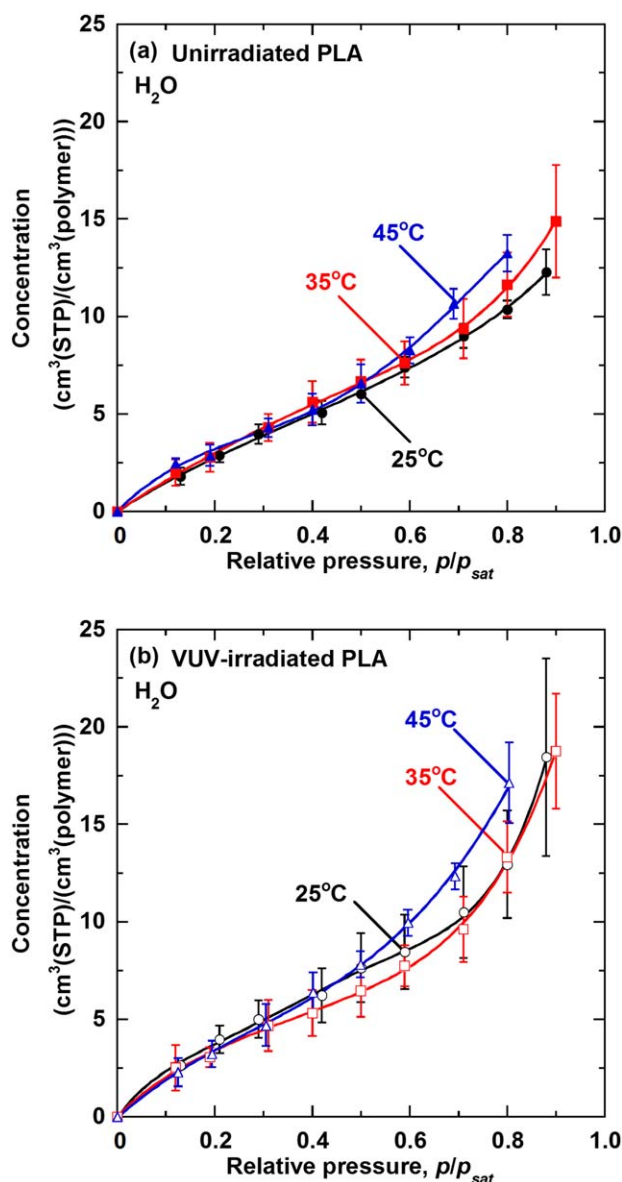
### Measurement of Water Vapor Sorption

Figure 3 shows the sorption isotherms for water in unirradiated [Figure 3(a)] and VUV-irradiated PLA films at 25, 35, and 45°C [Figure 3(b)]. The sorption isotherms of unirradiated and VUV-irradiated PLA films presented an S-shape. Film concentration initially increased as relative pressure increased, following the Langmuir adsorption, which is concave to the water vapor pressure axis. Film concentration then increased exponentially based on the Flory–Huggins behavior because the water molecules sorbed in the films caused swelling, plasticization of films, and clustering of water molecules.<sup>15,16</sup> The sorption isotherm shape was generally determined by gas or vapor solubility into polymers. When polymers are in a glassy state and the interaction between penetrants is strong, the sorption isotherm exhibits a gentle S-shaped curve. The glass transition temperature ( $T_g$ ) of PLA was 60.3°C.<sup>17</sup> PLA films are in a glassy state from 25 to 45°C. Therefore, the sorption isotherms depended on the Langmuir adsorption in low pressure and on PLA swelling and water vapor aggregation in high pressure. Comparing to nontreated and irradiated films, VUV-irradiated PLA films exhibited higher concentrations than unirradiated PLA films at high pressure.

The solubility coefficient of water vapor in the polymer film is expressed by eq. (3):

$$S = \frac{C}{p} \quad (3)$$

where  $S$  is the solubility coefficient [cm<sup>3</sup>(STP)/(cm<sup>3</sup>(polymer) cm Hg)]. Figure 4 shows the solubility coefficient for water in unirradiated [Figure 4(a)] and VUV-irradiated PLA films [Figure 4(b)] at 25, 35, and 45°C. As relative pressure increased, the solubility coefficients of water vapor in unirradiated PLA films initially decreased based on the Langmuir model in the low-pressure region ( $p/p_{\text{sat}} = 0.1\text{--}0.3$ ) and increased based on the Flory–Huggins behavior in the high-pressure region ( $p/p_{\text{sat}} = 0.7\text{--}0.9$ ). Solubility at low temperature was higher than that at high temperature, and the same behavior was observed in VUV-irradiated PLA films. However, the solubility of VUV-irradiated PLA films was higher than that of unirradiated PLA films close to the low-pressure region [10.9 ± 9.0% (25°C), 18.3 ± 7.9% (35°C), and 42.7 ± 5.33% (45°C)] and the high-pressure region [37.6 ± 12.6% (25°C), 20.2 ± 5.8% (35°C), and 30.9 ± 0.3% (45°C)]. The first solubility decrease of the glassy polymer in the low-pressure region resulted from the void



**Figure 3.** Sorption isotherms of water in (a) unirradiated PLA films at 25°C (•), 35°C (■), and 45°C (▲), and (b) VUV-irradiated PLA films at 25°C (○), 35°C (□), and 45°C (△). [Color figure can be viewed in the online issue, which is available at [wileyonlinelibrary.com](http://wileyonlinelibrary.com).]

decrease of adsorbed penetrants. Langmuir adsorption after VUV irradiation was increased by the affinity to water. In contrast, the solubility increase in the high-pressure region resulted from penetrant aggregation (clustering) by the polarity of molecules. Solubility parameters were calculated as indicators of affinity to determine the force of interaction between PLA and water. Polymer solubility is estimated using the calculated solubility parameters and group contribution method.<sup>17</sup> Solubility parameters are generally considered as approximate indicators of polymer solubility. PLA solubility was analyzed using the Hansen solubility parameter (HSP), which was determined by three parameters: (1) energy from dispersion bonds between molecules, (2) dipolar intermolecular force between molecules, and (3) hydrogen bonds between molecules. When the solubility

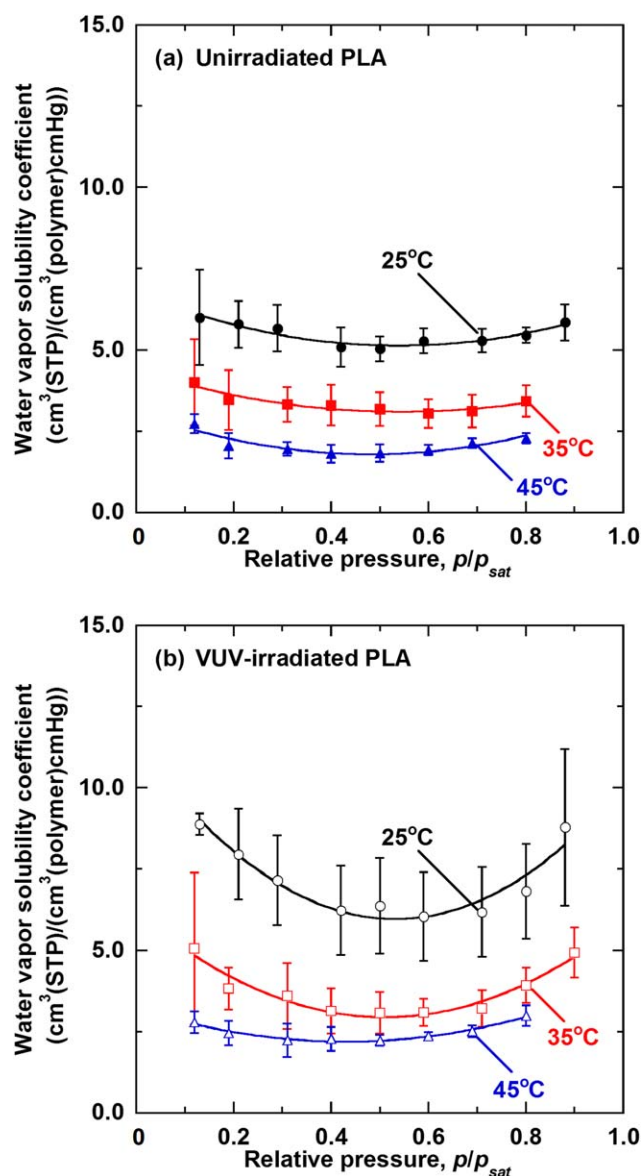


**Figure 4.** Solubility coefficients of water in (a) unirradiated PLA films at 25°C (•), 35°C (■), and 45°C (▲), and (b) VUV-irradiated PLA films at 25°C (○), 35°C (□), and 45°C (△). [Color figure can be viewed in the online issue, which is available at [wileyonlinelibrary.com](http://wileyonlinelibrary.com).]

parameter of the penetrant is close to the polymer, the affinity between the penetrant and polymer strengthens. The total HSP ( $\delta_t$ ) of PLA was 21.2 MPa<sup>1/2</sup>, and the  $\delta_t$  of water was 47.9 MPa<sup>1/2</sup>. A significant gap was observed between PLA and water. Therefore, the affinity interaction of water–PLA was weak in unirradiated PLA, and solubility increase was not caused by affinity. In contrast, VUV-irradiated PLA increased the interaction, and solubility was affected by the clustering of water molecules. Therefore, we analyzed the clustering function to examine the effects of the water–PLA interaction and state of water molecules in PLA films.

#### Analysis of Clustering

Clusters of water molecules are formed by self-hydrogen bonds between hydroxyl groups. We investigate the clustering of water

molecules. Clustering in polymer films is expressed using the Zimm and Lundberg formulation:<sup>18,19</sup>

$$\frac{G_{11}}{V_1} = -\varphi_2 \left[ \frac{\partial(a_1/\varphi_1)}{\partial a_1} \right]_{p,T} - 1 \quad (4)$$

where  $G_{11}$  represents the cluster integral;  $V_1$  is the partial molar volume of the water molecule;  $\varphi_1$  and  $\varphi_2$  are the volume fractions of the water molecule and polymer, respectively; and  $a_1$  is the activity of water molecules.  $a_1$  at a given activity is determined from the equilibrium sorption isotherm using this equation:

$$\varphi_1 = \frac{vR}{1+vR} \quad (5)$$

where  $v$  is the ratio of polymer density and water molecule and  $R$  [g/g(polymer)] is the equilibrium sorption regain.<sup>12,16</sup> Clustering functions have values of minus one for pure, condensed systems. In a pure system, a molecule excludes another molecule from its own molecular volume but has no other effect on the system. A clustering function that decreases without bound corresponds to a segregation function that increases without bound. The infinite segregation of like molecules is physically unreasonable even in the limits of zero concentrations. Therefore, clustering functions should be finite in the limits of zero concentrations. Figure 5 presents the clustering function  $G_{11}/V_1$  determined from the water vapor sorption isotherm of PLA as a function of water vapor activity. The  $G_{11}/V_1$  of both PLA films was less than minus one in the low activity range and more than minus one in the high activity range. Therefore, a large affinity exists between water–PLA dispersed water molecules in the low-pressure region. In contrast, the interactions between water molecules were strong in the high-pressure region. The  $G_{11}/V_1$  of unirradiated PLA films exhibited no temperature changes. However, the value of VUV-irradiated PLA films at 25 and 35°C decreased in the low-activity area and increased in the high-activity area because of solubility. The product of cluster function and volume fraction  $\varphi_1 G_{11}/V_1$  is a measure of the mean number of water molecules in the neighborhood of a given water molecule in excess of the mean concentration of penetrants in the polymer.<sup>18,20</sup> Therefore, mean cluster size (MCS) is calculated from  $\varphi_1 G_{11}/V_1 + 1$ . Figure 6 presents the MCS determined from the water vapor sorption isotherm of PLA as a function of water vapor activity. The MCS value was more one, which suggested that water molecules were clustered (i.e.,  $\varphi_1 G_{11}/V_1 > 0$ ). Table I summarizes the activity of each PLA film at the clustering point and MCS of water at maximum pressure ( $p/p_{\text{sat}} = 0.8\text{--}0.9$ ). Water in VUV-irradiated PLA was clustered at lower activity than in unirradiated PLA. The MCS of water at maximum pressure in VUV-irradiated PLA was roughly 1.4 times larger than that of unirradiated PLA, which indicated that water molecules were clustered in the PLA films at high pressure. The water molecules formed a huge cluster because solubility in the high-pressure region was increased by VUV irradiation, which then increased the water concentration in the film. Given that the cluster size of water molecules in the VUV-irradiated film increased, the huge cluster weakened the interaction between polymer chains, and the swelling effects increased solubility.

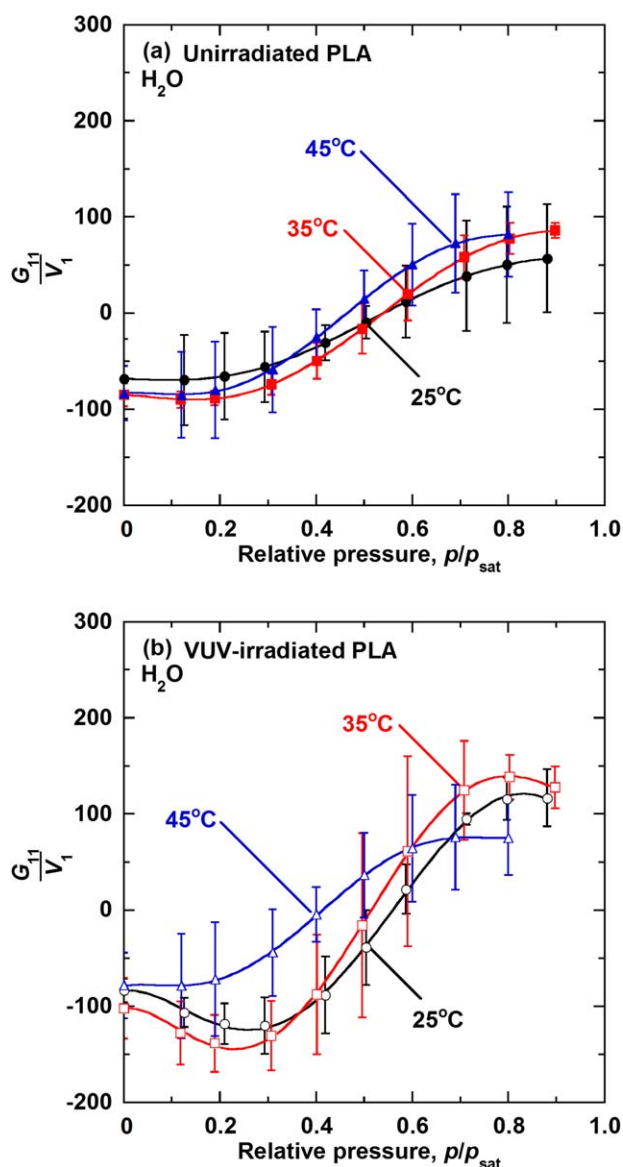


**Figure 5.** Zimm-Lundberg's clustering formations of water vapor in (a) unirradiated PLA films at 25°C (•), 35°C (■), and 45°C (▲), and (b) VUV-irradiated PLA films at 25°C (○), 35°C (□), and 45°C (△). [Color figure can be viewed in the online issue, which is available at [wileyonlinelibrary.com](http://wileyonlinelibrary.com).]

### Characterization Analysis

Changes in the film structure were observed by measuring the properties of PLA films before and after sorption. Figure 7 shows the WAXD patterns of PLA films before and after sorption measurement. Sharp peaks were not observed in the PLA film, and a halo was observed in the  $d$ -spacing of unirradiated PLA at  $5.3 \pm 0.1$  Å and VUV-irradiated PLA at  $5.3 \pm 0.2$  Å. Given that the  $d$ -spacing values presented no significant difference between unirradiated and VUV-irradiated films, VUV irradiation did not affect the internal film structure and only modified the shallow part near the surface. Therefore, VUV irradiation changes the surface structure and increases hydrophilicity, while maintaining the internal film structure.

SEM observation was conducted on the film surface and cross-section to clarify the internal state and modified surface after water vapor sorption. Figure 8 shows the SEM images of unirradiated and VUV-irradiated PLA films (surface and cross-section). In the SEM observation before sorption, the surface and cross-section of unirradiated PLA films were smooth before and after sorption measurements. In contrast, irregularities in PLA crystal growth branched out in a radial fashion in VUV-irradiated PLA films, and some cracks from photolysis were observed on the surface. In the film cross-section, the modified layer with a thickness of 2 to 3  $\mu\text{m}$  was observed near the surface. In the SEM observation after sorption, several defects were

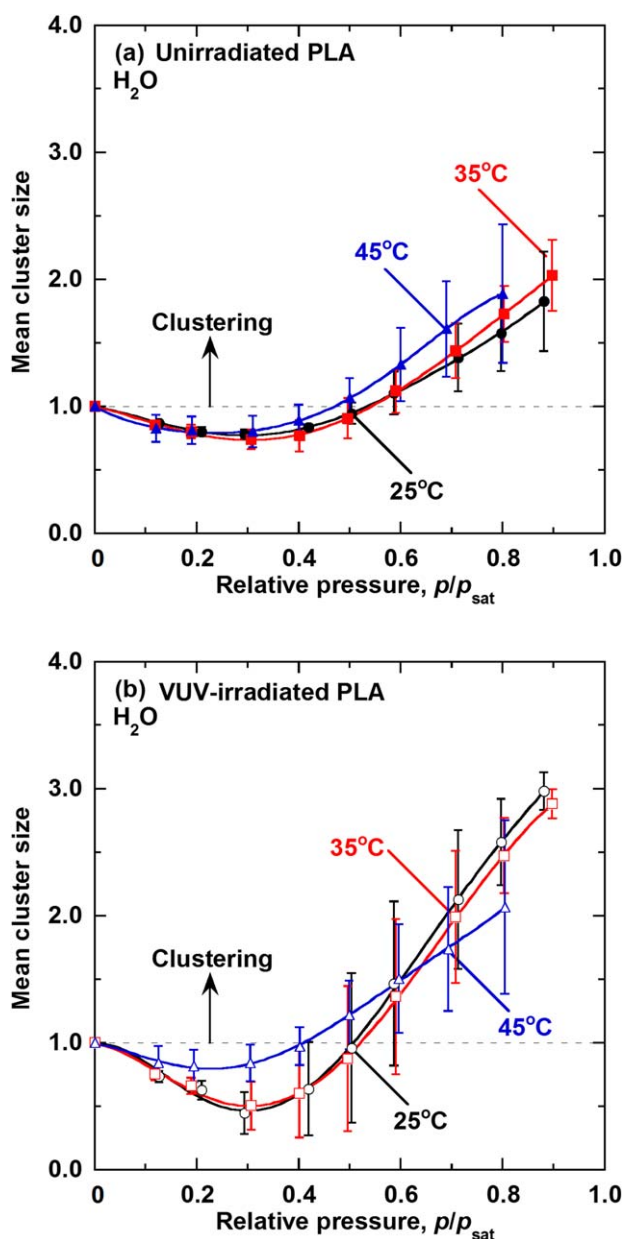


**Figure 6.** The mean cluster size of water molecules in (a) unirradiated PLA films at 25°C (•), 35°C (■), and 45°C (▲), and (b) VUV-irradiated PLA films at 25°C (○), 35°C (□), and 45°C (△). [Color figure can be viewed in the online issue, which is available at [wileyonlinelibrary.com](http://wileyonlinelibrary.com).]

**Table I.** Parameters of Clustering Water Vapor in PLA Films Before and After Irradiation

Sample	Temperature (°C)	Clustering point	Mean cluster size $p/p_{\text{sat}} > 0.8$
Unirradiated PLA	25	$0.59 \pm 0.11$	$1.83 \pm 0.39$
Unirradiated PLA	35	$0.54 \pm 0.08$	$2.03 \pm 0.28$
Unirradiated PLA	45	$0.46 \pm 0.10$	$1.89 \pm 0.55$
VUV-irradiated PLA	25	$0.50 \pm 0.14$	$2.98 \pm 0.15$
VUV-irradiated PLA	35	$0.50 \pm 0.14$	$2.88 \pm 0.11$
VUV-irradiated PLA	45	$0.41 \pm 0.13$	$2.07 \pm 0.68$

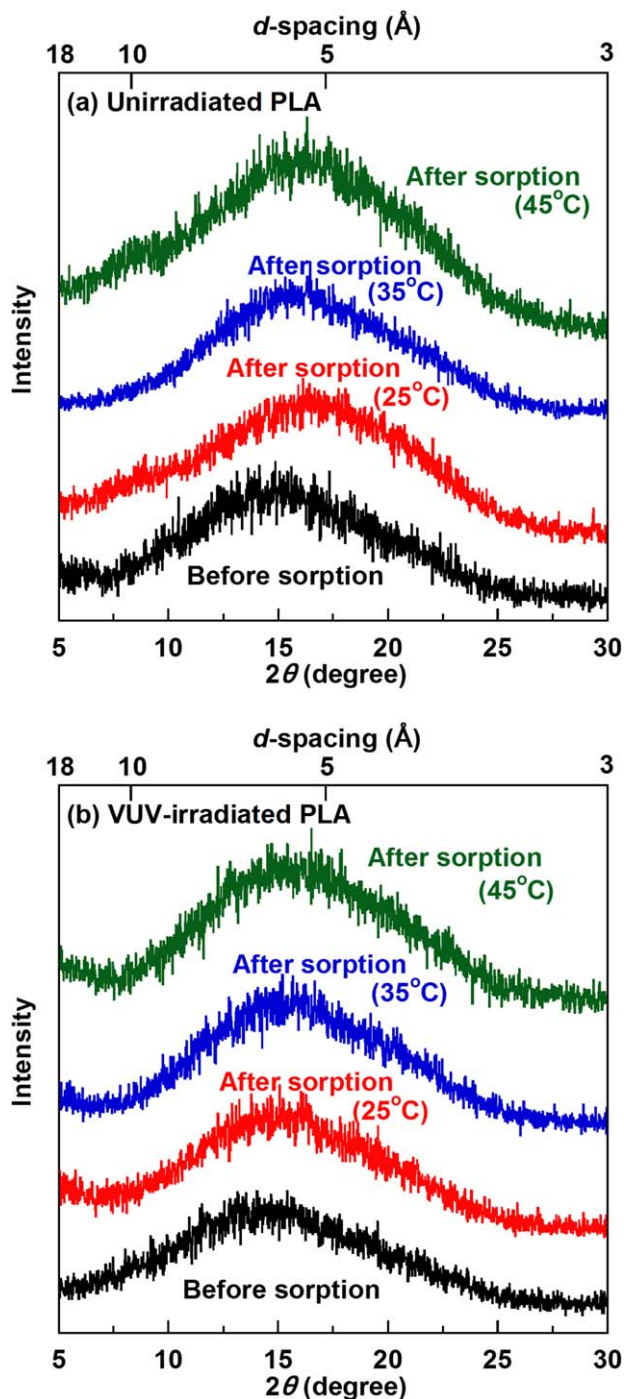
observed on one side of the VUV-irradiated surface. The missing part of awkward shapes was observed along mesh irregularities. VUV irradiation did not affect the inner part of the PLA film. We previously reported that the crystallinity of the PLA film surface is increased by VUV irradiation.<sup>4</sup> The film crystal structure was observed with transmitted light using POM. In the POM observation (Figure 9), although no color change was observed in unirradiated PLA, 2 to 3  $\mu\text{m}$  domain of polarization presented the crystal structure in VUV-irradiated PLA. Yellow and blue polarized light were observed in the PLA film after water vapor sorption, but there was no polarized light inside the defect portion. The polarization observed in VUV-irradiated PLA films before water vapor sorption indicated a density difference and crystal film with uneven swelling in the modified layer. Therefore, the thicknesses of the modified layer and defects were assumed to be approximately 2–3  $\mu\text{m}$  from the surface. The internal part was not modified by VUV irradiation. Crystalline parts were observed, which the hydrophilic polymer chains aggregated in the modified layer of PLA; the layer was non-uniformly swelling after water vapor sorption. The results of excessive surface swelling increased water vapor solubility.

Figure 10 presents the ATR spectra of O–H stretching for both PLA films before and after sorption.

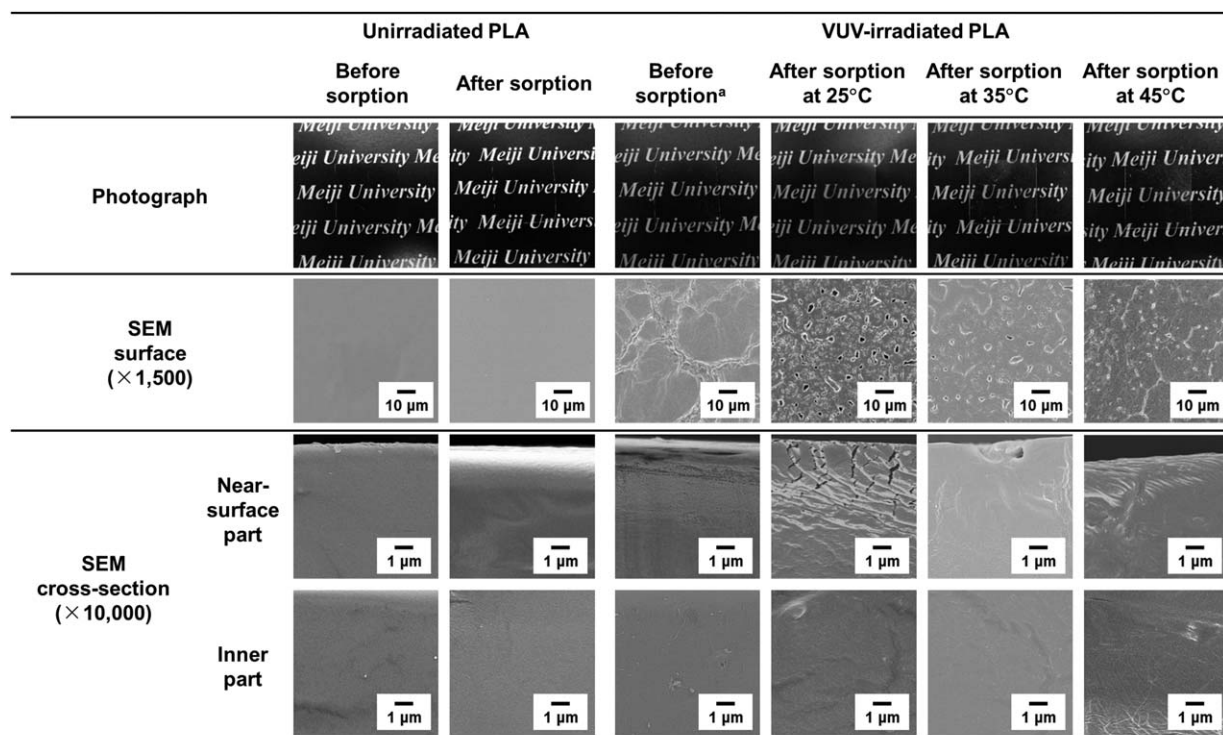
PLA: ATR-FTIR; 2995  $\text{cm}^{-1}$  and 2945  $\text{cm}^{-1}$  (C–H stretching), 1755  $\text{cm}^{-1}$  (C=O stretching), 1180  $\text{cm}^{-1}$  (C–O–C stretching), 1450  $\text{cm}^{-1}$  (C–H stretching, C–H bending), 1640  $\text{cm}^{-1}$  (C=C stretching).

The ATR spectra obtained showed the appearance of cleaved PLA peak (C=C stretching) at 1640  $\text{cm}^{-1}$ . No O–H stretching peaks were observed before and after sorption in the unirradiated PLA films. In contrast, a broad peak was observed from 3200 to 3600  $\text{cm}^{-1}$  in VUV-irradiated PLA films after water vapor exposure. The other side of the irradiated surface showed the same spectrum as the unirradiated PLA. Three general types of water molecule structures existed: nonfreezing, freezing bound, and freezing. Morita *et al.* reported the hydration structure analysis of poly(2-methoxyethylacrylate) based on the ATR spectra from 3100 to 3800  $\text{cm}^{-1}$  (O–H stretching).<sup>21</sup> According to literature, the peak of O–H stretching vibration near

3600  $\text{cm}^{-1}$  represented nonfreezing water and indicated the hydrogen bonding of carbonyl and hydroxyl groups. Another peak near 3400  $\text{cm}^{-1}$  represented freezing bound water and indicated the interaction between hydroxyl and methoxy groups of the side chains. The O–H stretching vibration peak observed from 3200 to 3400  $\text{cm}^{-1}$  represented freezing water, which induced bulk water. The chemical structure that corresponded



**Figure 7.** WAXD spectra of (a) unirradiated PLA films and (b) VUV-irradiated PLA films before and after water vapor sorption. [Color figure can be viewed in the online issue, which is available at [wileyonlinelibrary.com](http://wileyonlinelibrary.com).]



<sup>a</sup> SEM image for the surface of VUV-irradiated PLA before sorption was quoted from reference.<sup>4</sup>

**Figure 8.** Photographs and SEM images of unirradiated and VUV-irradiated PLA films before and after water vapor sorption.

to their peak analysis is the same as that of PLA. Therefore, the peak at roughly  $3500\text{ cm}^{-1}$  is attributed to the strong interaction of nonfreezing and freezing bound water to the surface of VUV-irradiated PLA. Carboxyl groups were generated in the irradiated surface layer of PLA by Norrish type II reaction. Consequently, water molecules were almost nonexistent in the unirradiated surface. In contrast, water molecules were observed on

the surface of VUV-irradiated films, which exhibited strong hydrogen bonds with the polymer chain. Therefore, hydrophilicity increased and swelling occurred only at the surface of the modified layer because of the strong bond between the water molecules and modified layer. Swelling increased the cluster size, and the solubility coefficient of PLA film increased after VUV irradiation.

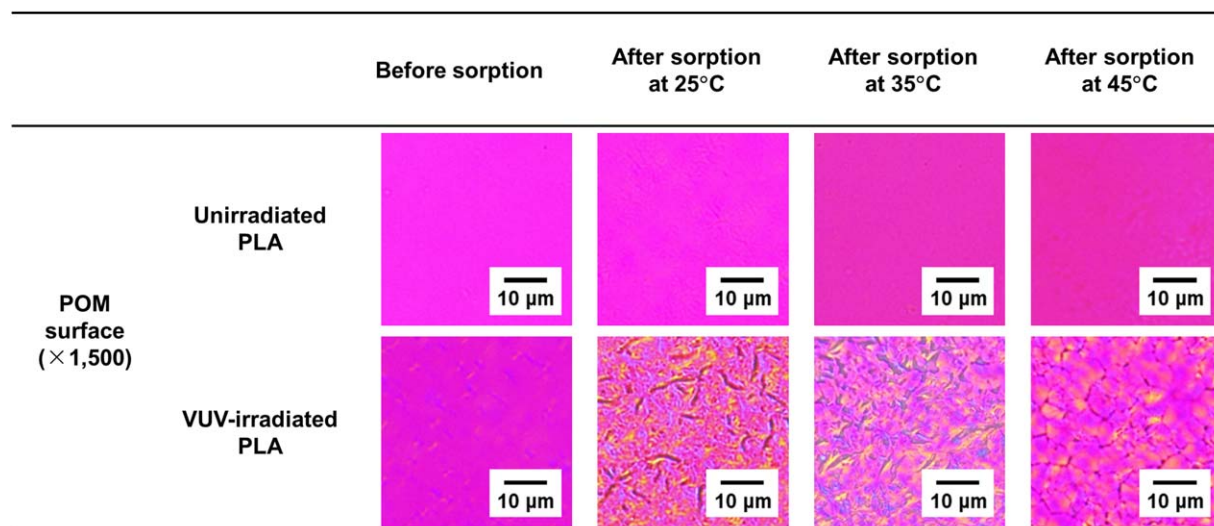


**Figure 9.** POM images of unirradiated and VUV-irradiated PLA films before and after water vapor sorption. [Color figure can be viewed in the online issue, which is available at [wileyonlinelibrary.com](http://wileyonlinelibrary.com).]

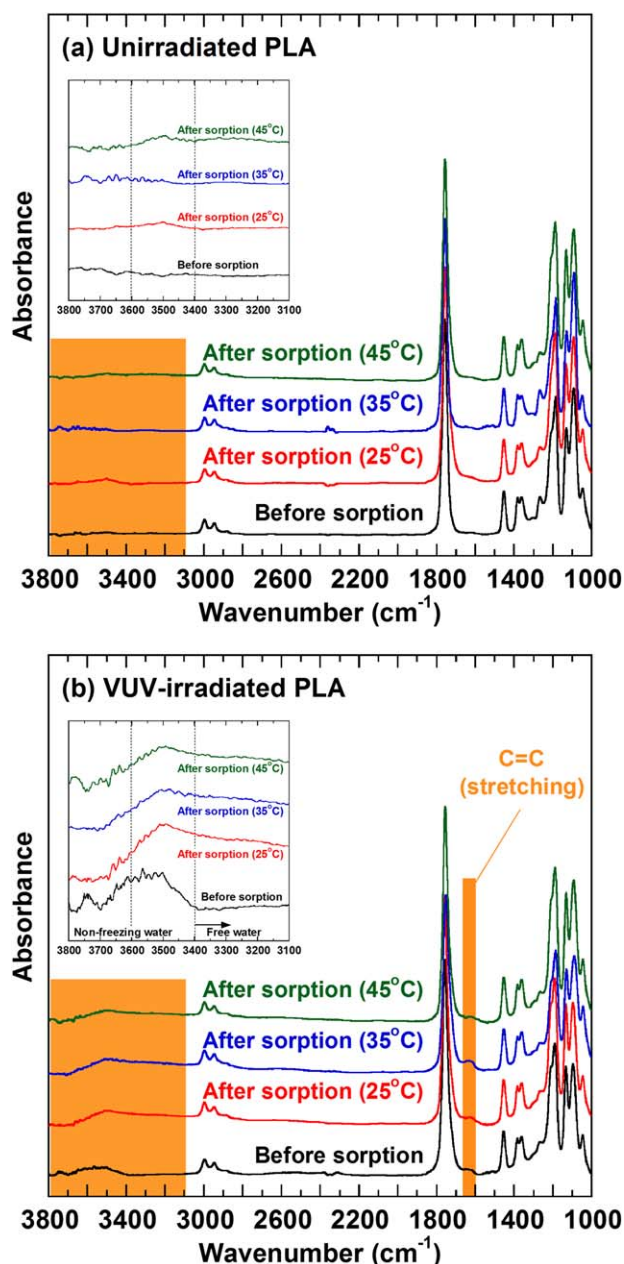


**Figure 10.** ATR-FTIR spectra of (a) unirradiated PLA films and (b) VUV-irradiated PLA films before and after water vapor sorption. [Color figure can be viewed in the online issue, which is available at [wileyonlinelibrary.com](http://wileyonlinelibrary.com).]

## CONCLUSIONS

Surface modification of PLA film was performed using 172 nm excimer lamp irradiation. The effects of VUV irradiation on water vapor solubility and physical properties were studied systematically. Water vapor solubility of PLA had the same characteristics as typical glassy polymer. Water vapor solubility increased after VUV irradiation of PLA, which we observed in both ends of the low-pressure and high-pressure regions. Water molecules were

absorbed in VUV-irradiated PLA, which formed huge clusters in the high-pressure region. The hydrophilic layer formed a thickness of 2–3  $\mu\text{m}$  from the irradiated surface via VUV irradiation, but there were no changes inside of the irradiated film. The crystalline structure formed in the modified surface layer through the aggregation of hydrophilic groups, and strong bonds were observed between the groups and water at the surface layer. Therefore, the modified layer absorbed a large amount of water because of the hydrophilic increase and was highly swollen. The solubility coefficient of PLA films after irradiation was increased by the effect of the modified hydrophilic surface.

## REFERENCES

- Sawada, H.; Takahashi, Y.; Miyata, S.; Kanehashi, S.; Sato, S.; Nagai, K. *Trans. Mater. Res. Soc. Jpn.* **2010**, *35*, 241.
- Truica-Marasescu, F.; Pham, S.; Wertheimer, M. R. *Nucl. Instrum. Methods Phys. Res. Sect. B* **2007**, *265*, 31.
- Ozdemir, M.; Yurteri, C. U.; Sadikoglu, H. *Crit. Rev. Food Sci. Nutr.* **1999**, *39*, 457.
- Sato, S.; Ono, M.; Yamauchi, J.; Kanehashi, S.; Ito, H.; Matsumoto, S.; Iwai, Y.; Matsumoto, H.; Nagai, K. *Desalination* **2012**, *287*, 290.
- Mathieson, I.; Bradley, R. H. *Int. J. Adhes. Adhes.* **1996**, *16*, 29.
- Vig, J. R. *J. Vac. Sci. Technol. A* **1985**, *3*, 1027.
- Ko, Y. G.; Kim, Y. H.; Park, K. D.; Lee, H. J.; Lee, W. K.; Park, H. D.; Kim, S. H.; Lee, G. S.; Ahn, D. J. *Biomaterials* **2001**, *22*, 2115.
- Jang, J.; Jeong, Y. *Dyes Pigment.* **2005**, *69*, 137.
- Ikada, E. *J. Photopolym. Sci. Technol.* **1993**, *6*, 115.
- Ikada, E. *J. Photopolym. Sci. Technol.* **1997**, *10*, 265.
- Nagai, K.; Sugawara, A.; Kazama, S.; Freeman, B. D. *J. Polym. Sci. Part B: Polym. Phys.* **2004**, *42*, 2407.
- Kanehashi, S.; Konishi, S.; Takeo, K.; Owa, K.; Kawakita, H.; Sato, S.; Miyakoshi, T.; Nagai, K. *J. Membr. Sci.* **2013**, *427*, 176.
- Poling, B. E. *The Properties of Gases and Liquids*; New York: McGraw-Hill, **2001**.
- Dixon-Garrett, S. V.; Nagai, K.; Freeman, B. D. *J. Polym. Sci. Part B: Polym. Phys.* **2000**, *38*, 1078.
- Mauze, G. R.; Stern, S. A. *J. Membr. Sci.* **1984**, *18*, 99.
- Kelkar, A. J. and Paul, D. R. *J. Membr. Sci.* **2001**, *181*, 199.
- Sato, S.; Gondo, D.; Wada, T.; Kanehashi, S.; Nagai, K. *J. Appl. Polym. Sci.* **2013**, *129*, 1607.
- Lundberg, J. L. *Pure Appl. Chem.* **1972**, *31*, 261.
- Zimm, B. H. *J. Chem. Phys.* **1953**, *21*, 934.
- Detallante, V.; Langevin, D.; Chappey, C.; Metayer, M.; Mercier, R.; Pineri, M. *J. Membr. Sci.* **2001**, *190*, 227.
- Morita, S.; Tanaka, M.; Ozaki, Y. *Langmuir* **2007**, *23*, 3750.